

Solvent responses and substituent effects upon magnetic properties of mononuclear Dy^{III} compounds

Sheng Zhang,^{*a} Nan Shen,^a Jiangwei Zhang,^{*b} Fang Xu,^a Jin Zhang,^a Jiamin Tang,^a Dengwei Hu,^a Bing Yin,^{*c} Sanping Chen^{*c}

AUTHOR ADDRESS

- a. Faculty of Chemistry and Chemical Engineering, Engineering Research Center of Advanced Ferroelectric Functional Materials, Key Laboratory of Phytochemistry of Shaanxi Province, Baoji University of Arts and Sciences, 1 Hi-Tech Avenue, Baoji, Shaanxi, 721013, China
 - b. State Key Laboratory of Catalysis, Dalian Institute of Chemical Physics, Chinese Academy of Sciences (CAS) Dalian 116023, P.R.China
 - c. Key Laboratory of Synthetic and Natural Functional Molecule Chemistry of Ministry of Education, College of Chemistry and Materials Science, Northwest University, Xi'an, Shaanxi 710069, China
-

Corresponding Authors

*E-mail: zhangsheng19890501@163.com. (S. Zhang)

*E-mail: jwzhang@dicp.ac.cn. (J.-W. Zhang)

*E-mail: rayinyin@nwu.edu.cn. (B. Yin)

*E-mail: sanpingchen@126.com (S.-P. Chen)

Table S1 Bond lengths and bond angles for **1**.

Atom	Atom	Length/Å	
Dy1	O1	2.239(3)	
Dy1	O2	2.315(3)	
Dy1	O3	2.326(3)	
Dy1	O4	2.275(3)	
Dy1	N1	2.531(3)	
Dy1	N2	2.666(3)	
Dy1	N3	2.658(3)	
Dy1	N4	2.565(3)	
Atom	Atom	Atom	Angle/°
O1	Dy1	O2	79.10(10)
O1	Dy1	O3	103.11(11)
O1	Dy1	O4	150.72(10)
O1	Dy1	N1	74.62(10)
O1	Dy1	N2	89.83(10)
O1	Dy1	N3	74.23(10)
O1	Dy1	N4	131.62(11)
O2	Dy1	O3	71.95(10)
O2	Dy1	N1	137.28(11)
O2	Dy1	N2	146.15(10)
O2	Dy1	N3	77.27(10)
O2	Dy1	N4	69.59(11)
O3	Dy1	N1	81.90(11)
O3	Dy1	N2	141.89(11)
O3	Dy1	N3	148.99(11)
O3	Dy1	N4	101.08(11)
O4	Dy1	O2	127.14(10)
O4	Dy1	O3	77.45(12)
O4	Dy1	N1	76.53(10)
O4	Dy1	N2	74.36(10)
O4	Dy1	N3	120.14(11)
O4	Dy1	N4	75.51(11)
N1	Dy1	N2	67.04(11)
N1	Dy1	N3	125.17(10)
N1	Dy1	N4	150.45(11)
N3	Dy1	N2	68.92(11)
N4	Dy1	N2	96.14(11)
N4	Dy1	N3	63.72(11)

Table S2 Bond lengths and bond angles for **2**.

Atom	Atom	Length/Å
Dy1	O1	2.330(3)
Dy1	O2	2.308(3)
Dy1	O3	2.226(3)

Dy1	O4	2.269(4)	
Dy1	N1	2.647(4)	
Dy1	N2	2.595(4)	
Dy1	N3	2.598(4)	
Dy1	N4	2.633(4)	
Atom	Atom	Atom	Angle/ ^o
O1	Dy1	N1	77.45(13)
O1	Dy1	N2	141.57(13)
O1	Dy1	N3	69.67(13)
O1	Dy1	N4	147.27(13)
O2	Dy1	O1	71.73(12)
O2	Dy1	N1	147.98(13)
O2	Dy1	N2	77.68(13)
O2	Dy1	N3	112.06(14)
O2	Dy1	N4	140.84(13)
O3	Dy1	O1	121.92(13)
O3	Dy1	O2	81.38(13)
O3	Dy1	O4	150.31(13)
O3	Dy1	N1	123.52(13)
O3	Dy1	N2	74.38(13)
O3	Dy1	N3	74.86(13)
O3	Dy1	N4	76.66(14)
O4	Dy1	O1	82.97(13)
O4	Dy1	O2	93.16(14)
O4	Dy1	N1	74.38(14)
O4	Dy1	N2	75.94(14)
O4	Dy1	N3	133.17(13)
O4	Dy1	N4	90.31(14)
N2	Dy1	N1	125.29(14)
N2	Dy1	N3	145.73(13)
N2	Dy1	N4	65.41(14)
N3	Dy1	N1	63.25(14)
N3	Dy1	N4	93.02(14)
N4	Dy1	N1	69.90(14)

Table S3 Bond lengths and bond angles for **3**.

Atom	Atom	Length/Å
Dy1	O1	2.249(3)
Dy1	O2	2.298(3)
Dy1	O3	2.277(3)
Dy1	O4	2.328(3)
Dy1	N1	2.647(3)
Dy1	N2	2.662(3)
Dy1	N3	2.521(3)
Dy1	N4	2.574(3)

Atom	Atom	Atom	Angle/°
O1	Dy1	O2	78.61(10)
O1	Dy1	O3	151.05(10)
O1	Dy1	O4	103.92(11)
O1	Dy1	N1	74.10(10)
O1	Dy1	N2	89.20(10)
O1	Dy1	N3	74.30(10)
O1	Dy1	N4	131.40(10)
O2	Dy1	O4	71.89(10)
O2	Dy1	N1	77.74(10)
O2	Dy1	N2	146.47(10)
O2	Dy1	N3	136.09(11)
O2	Dy1	N4	69.88(10)
O3	Dy1	O2	127.60(10)
O3	Dy1	O4	77.52(11)
O3	Dy1	N1	119.33(10)
O3	Dy1	N2	74.31(10)
O3	Dy1	N3	77.36(10)
O3	Dy1	N4	75.22(10)
O4	Dy1	N1	149.24(10)
O4	Dy1	N2	141.65(11)
O4	Dy1	N3	81.85(11)
O4	Dy1	N4	100.32(11)
N1	Dy1	N2	68.87(11)
N3	Dy1	N1	125.15(11)
N3	Dy1	N2	67.06(11)
N3	Dy1	N4	151.27(11)
N4	Dy1	N1	63.88(11)
N4	Dy1	N2	97.09(11)

Table S4 Bond lengths and bond angles for **4**.

Atom		Length/Å	
Dy1		2.309(4)	
Dy1		2.279(4)	
Dy1		2.321(4)	
Dy1		2.244(4)	
Dy1		2.663(5)	
Dy1		2.651(5)	
Dy1		2.533(5)	
Dy1		2.563(5)	
Atom	Atom	Atom	Angle/°
O1	Dy1	O3	72.04(14)
O1	Dy1	N1	142.46(15)
O1	Dy1	N2	148.42(15)
O1	Dy1	N3	82.79(15)

O1	Dy1	N4	101.12(16)
O2	Dy1	O1	77.20(17)
O2	Dy1	O3	127.13(14)
O2	Dy1	N1	74.67(14)
O2	Dy1	N2	120.71(15)
O2	Dy1	N3	76.66(15)
O2	Dy1	N4	75.45(16)
O3	Dy1	N1	145.49(14)
O3	Dy1	N2	76.62(14)
O3	Dy1	N3	137.81(15)
O3	Dy1	N4	69.80(16)
O4	Dy1	O1	102.58(16)
O4	Dy1	O2	151.12(15)
O4	Dy1	O3	78.40(15)
O4	Dy1	N1	90.73(14)
O4	Dy1	N2	74.37(14)
O4	Dy1	N3	74.68(15)
O4	Dy1	N4	131.62(16)
N2	Dy1	N1	68.89(14)
N3	Dy1	N1	66.95(15)
N3	Dy1	N2	124.74(14)
N3	Dy1	N4	150.15(16)
N4	Dy1	N1	95.36(15)
N4	Dy1	N2	63.61(15)

Table S5 Dy^{III} ion geometry analysis by SHAPE 2.1 software.

Configuration	ABOXIY, 1	ABOXIY, 2	ABOXIY, 3	ABOXIY, 4
Octagon(D8h)	31.968	32.232	31.892	32.093
Heptagonal pyramid(C7v)	22.017	21.727	22.324	21.957
Hexagonal bipyramid(D6h)	13.011	12.493	12.889	13.216
Cube(Oh)	7.245	8.261	7.027	7.340
Square antiprism (D_{4d})	3.247	2.611	3.035	3.374
Triangular dodecahedron (D_{2d})	0.601	1.108	0.613	0.572
Johnson gyrobifastigium J26 (D_{2d})	15.342	12.635	15.225	15.513
Johnson elongated triangular bipyramid J14 (D_{3h})	28.233	26.817	28.071	28.483
Biaugmented trigonal prism J50 (C_{2v})	3.271	2.076	3.507	3.194
Biaugmented trigonal prism (C_{2v})	3.196	2.061	3.109	3.152
Snub sphenoid J84 (D_{2d})	3.779	4.099	3.929	3.691
Triakis tetrahedron(Td)	8.014	9.032	7.761	8.126
Elongated trigonal bipyramid(D3h)	24.200	24.404	24.029	24.164

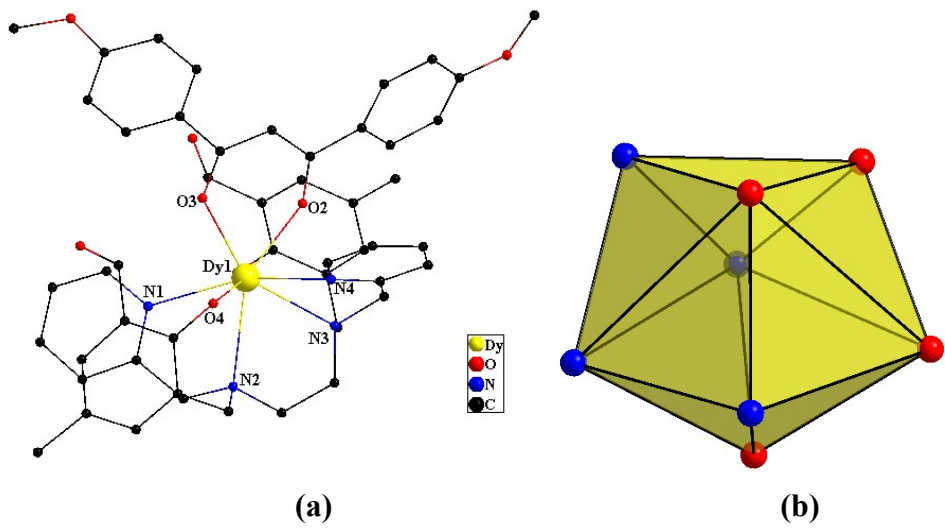


Fig. S1 The crystal structure of compound **1** (a) showing general ligand configurations.

Local coordination geometry of the Dy^{III} ion for compound **1** (b) (hydrogen atoms are omitted for clarity).

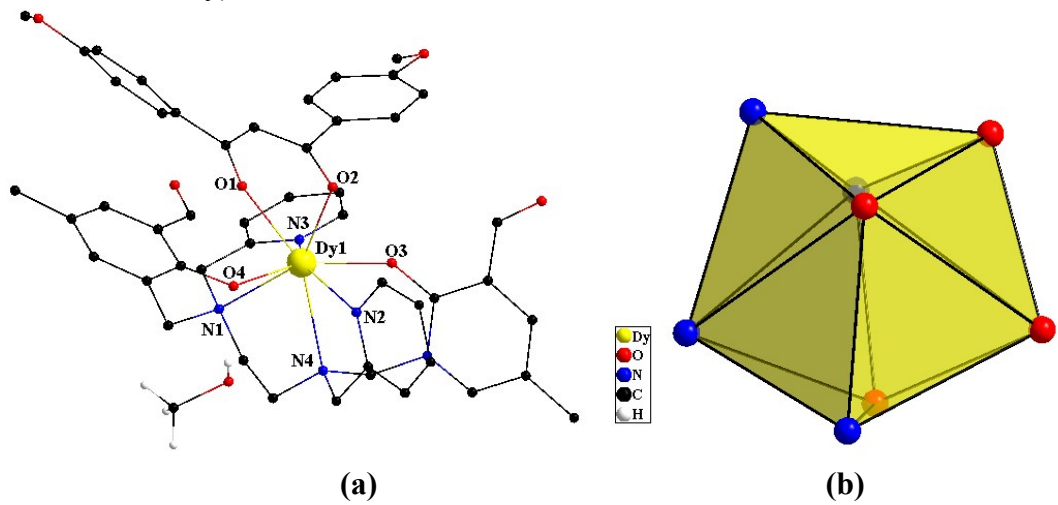


Fig. S2 The crystal structure of compound **2** (a) showing general ligand configurations.

Local coordination geometry of the Dy^{III} ion for compound **2** (b) (hydrogen atoms are omitted for clarity).

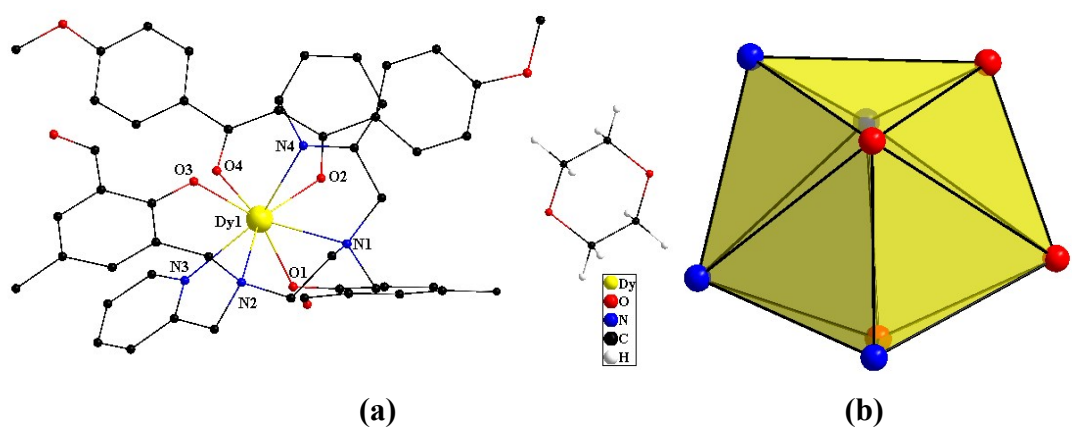


Fig. S3 The crystal structure of compound **3** (a) showing general ligand configurations.

Local coordination geometry of the Dy^{III} ion for compound **3** (b) (hydrogen atoms are omitted for clarity).

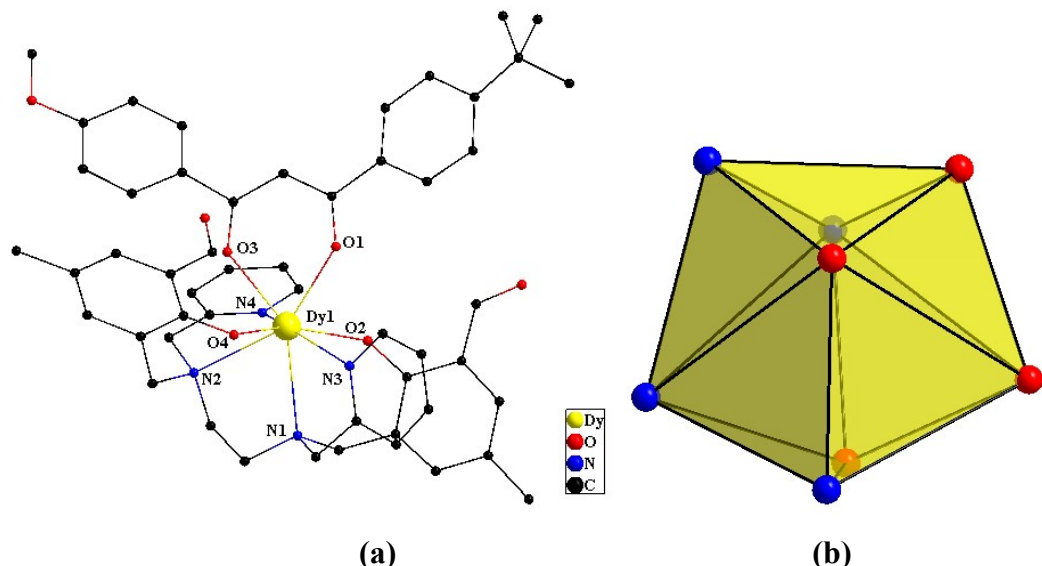


Fig. S4 The crystal structure of compound **4** (a) showing general ligand configurations.

Local coordination geometry of the Dy^{III} ion for compound **4** (b) (hydrogen atoms are omitted for clarity).

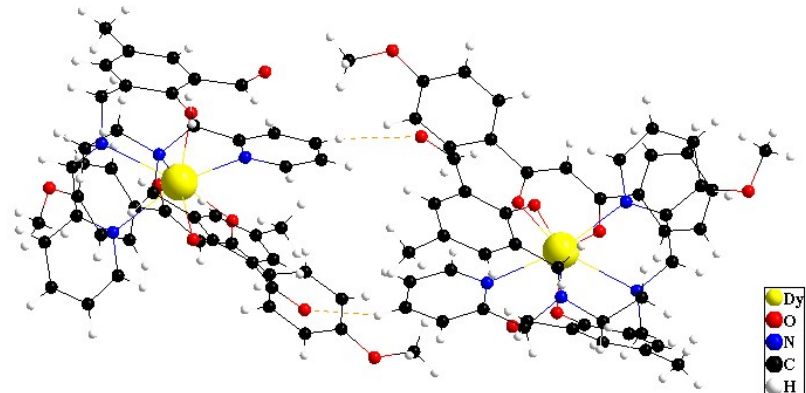


Fig. S5 The hydrogen bonding interactions in compound **1**. The yellow dotted lines represent C–H···O hydrogen bonding interactions.

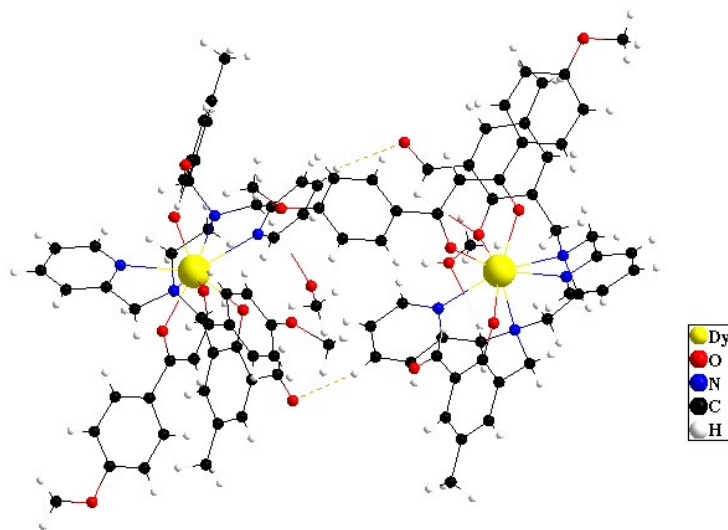


Fig. S6 The hydrogen bonding interactions in compound 2. The yellow dotted lines represent C–H···O hydrogen bonding interactions.

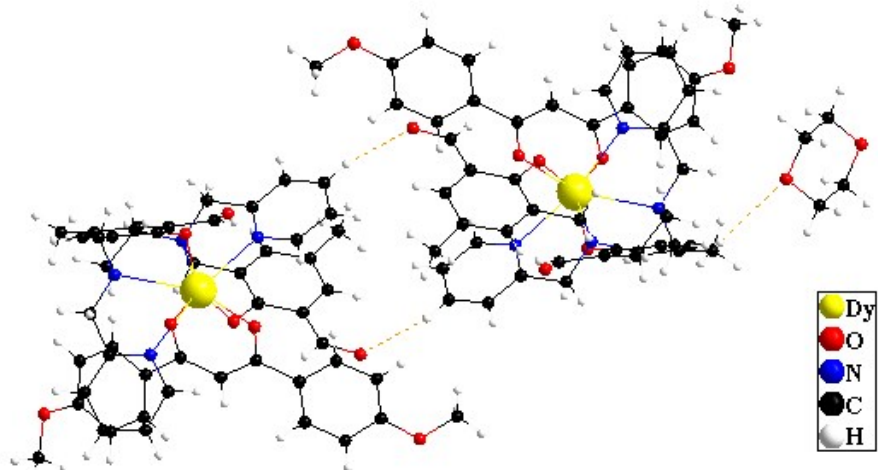


Fig. S7 The hydrogen bonding interactions in compound 3. The yellow dotted lines represent C–H···O hydrogen bonding interactions.

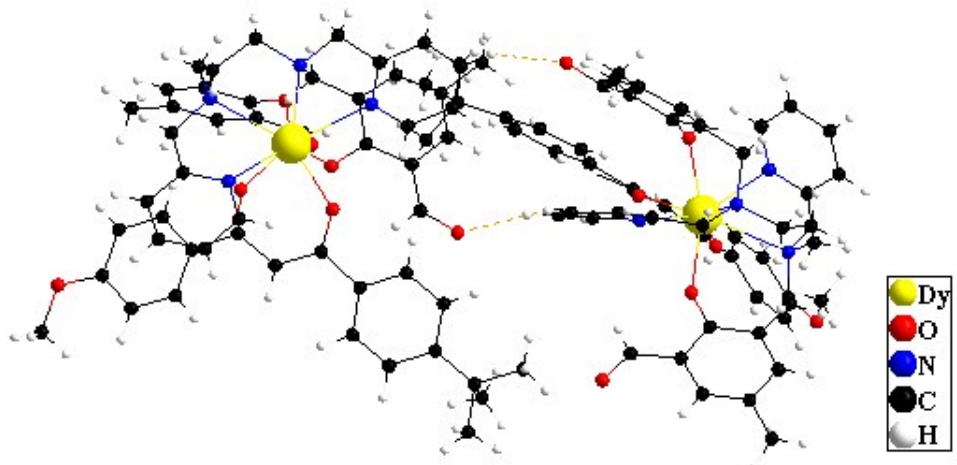


Fig. S8 The hydrogen bonding interactions in compound 4. The yellow dotted lines

represent C–H···O hydrogen bonding interactions.

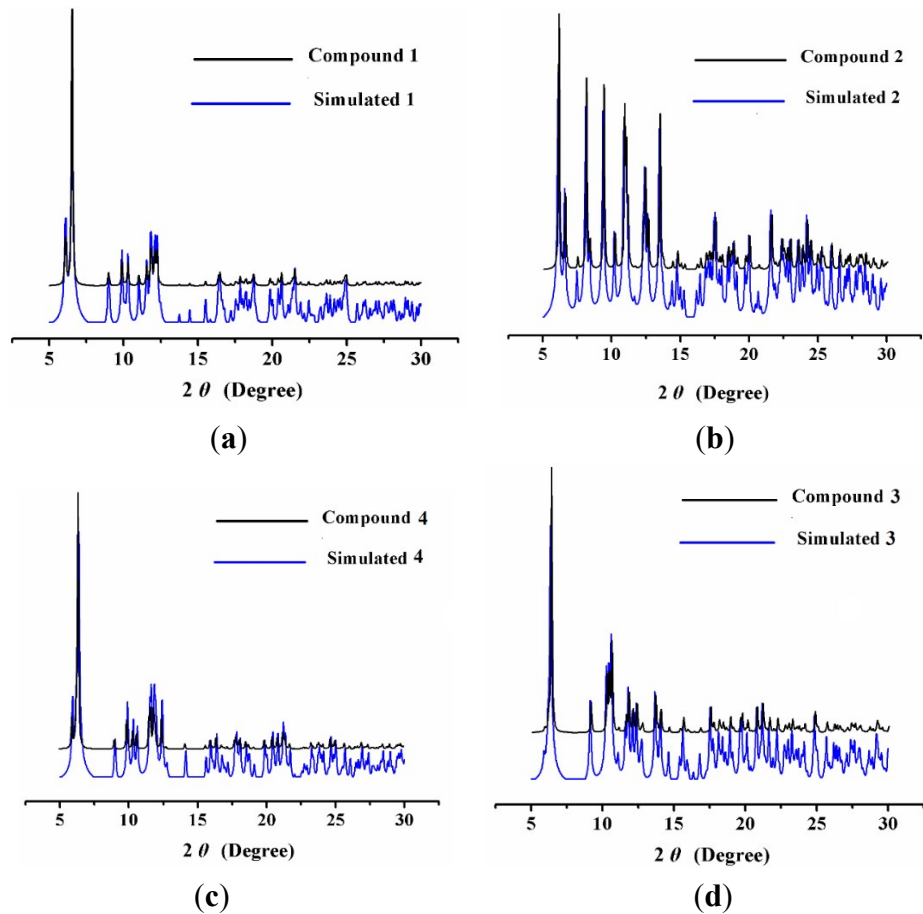
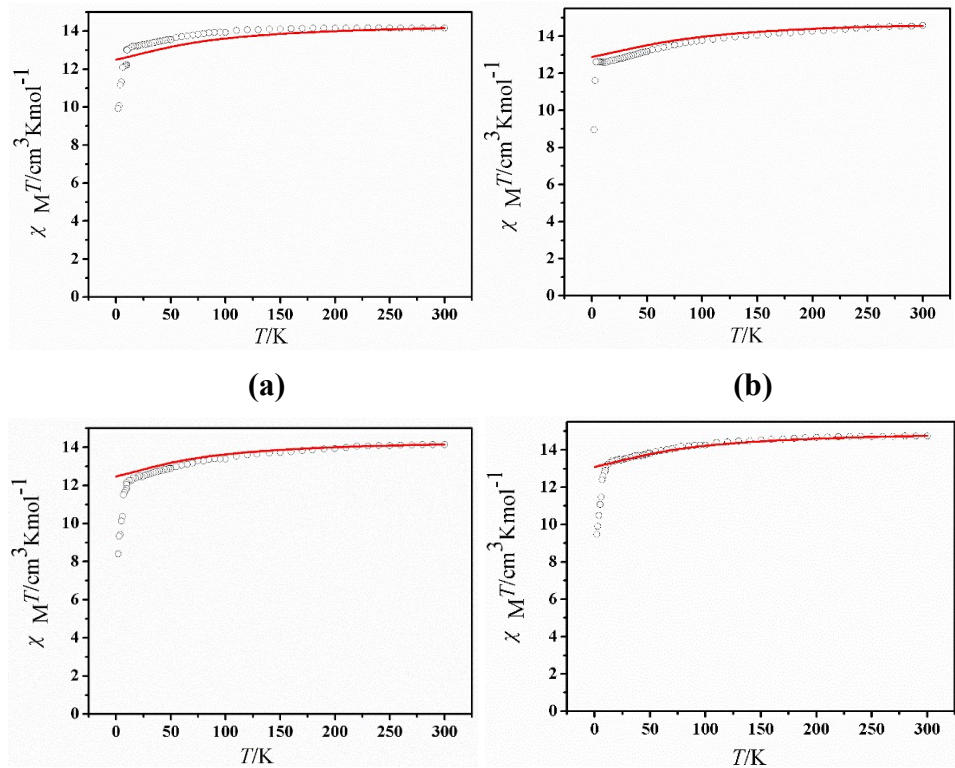


Fig. S9 XRPD curves of 1-4 (a-d).



(c) (d)

Fig. S10 Temperature dependence of $\chi_M T$ for **1-4** (a-d). The red lines represent the simulation from ab initio calculation.

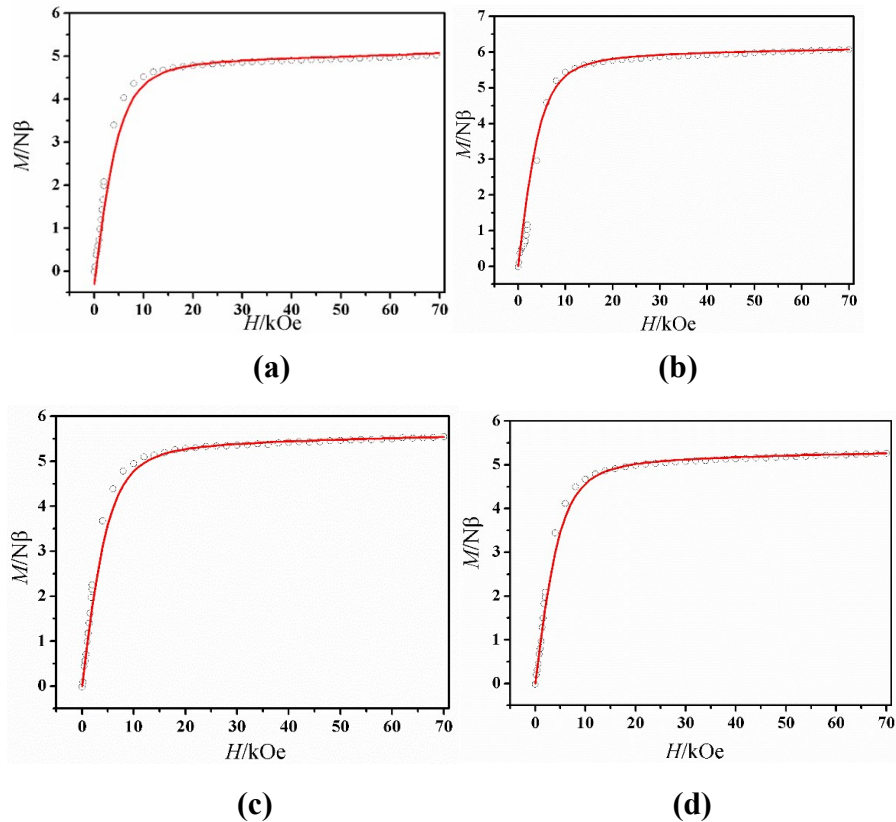


Fig. S11 $M(H)$ plots for **1-4** (a-d) between 0 and 70 kOe and at temperature of 2.0 K, respectively. The red lines represent the simulation from *ab initio* calculation.

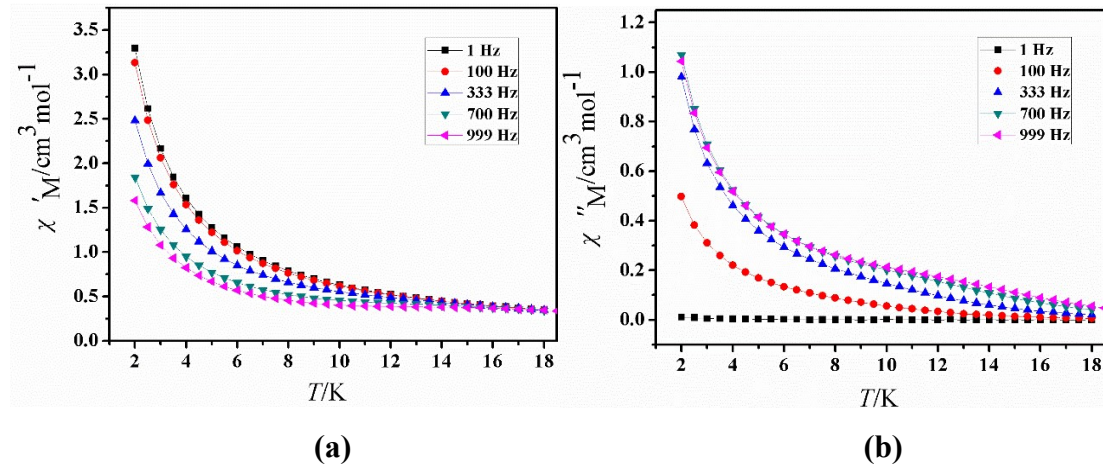


Fig. S12 Temperature dependence of the in-phase (χ' , a) and out-of-phase (χ'' , b) ac susceptibility signals under 0 Oe dc field for **1**.

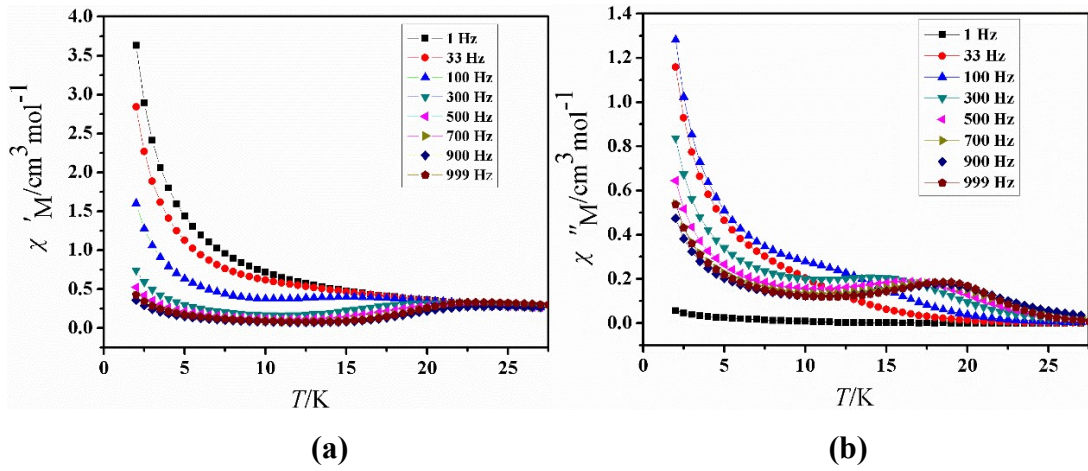


Fig. S13 Temperature dependence of the in-phase (χ' , a) and out-of-phase (χ'' , b) ac susceptibility signals under 0 Oe dc field for **2**.

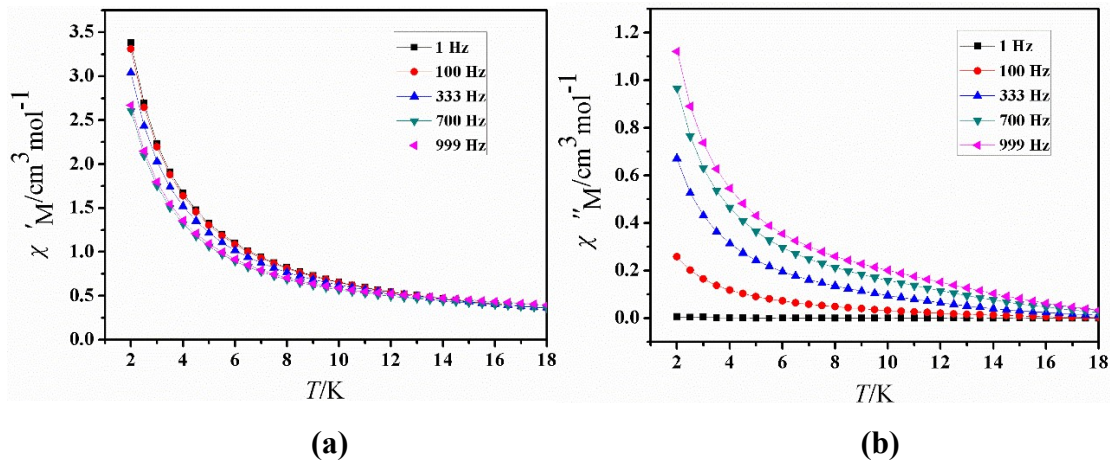


Fig. S14 Temperature dependence of the in-phase (χ' , a) and out-of-phase (χ'' , b) ac susceptibility signals under 0 Oe dc field for **3**.

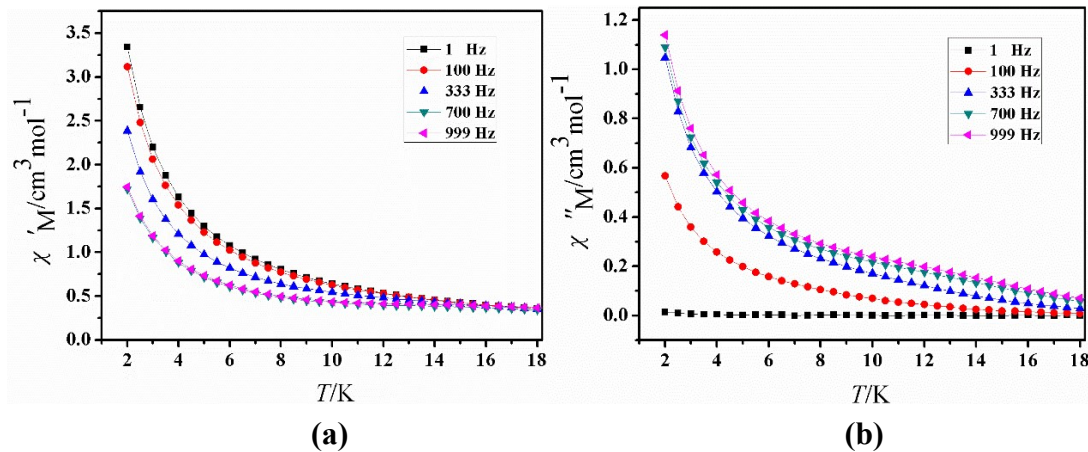


Fig. S15 Temperature dependence of the in-phase (χ' , a) and out-of-phase (χ'' , b) ac susceptibility signals under 0 Oe dc field for **4**.

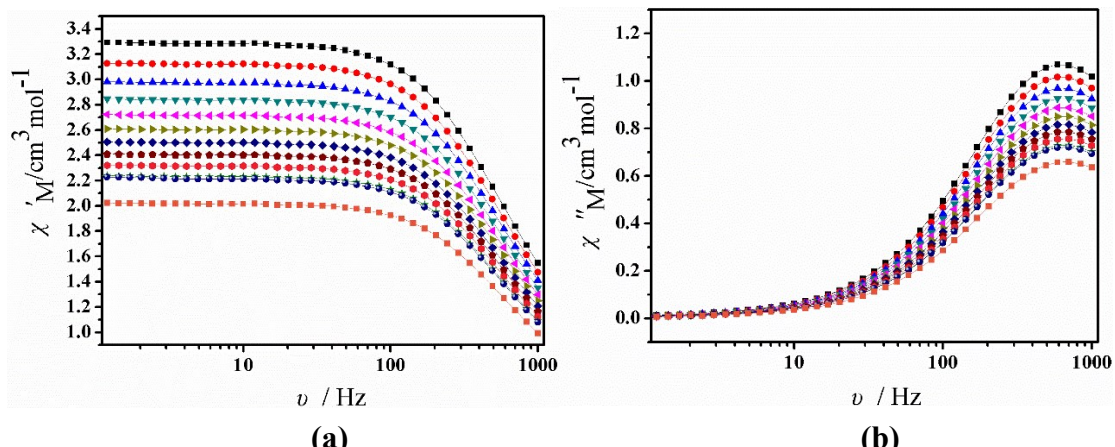


Fig. S16 Plots of the frequency-dependent in-phase (a) and out-of-phase (b) ac susceptibility at indicated temperatures for **1**.

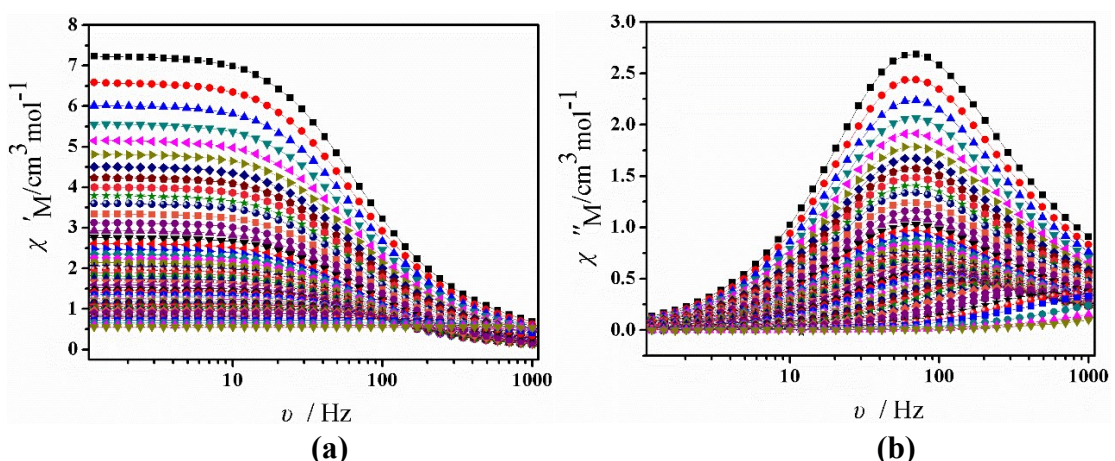


Fig. S17 Plots of the frequency-dependent in-phase (a) and out-of-phase (b) ac susceptibility at indicated temperatures for **2**.

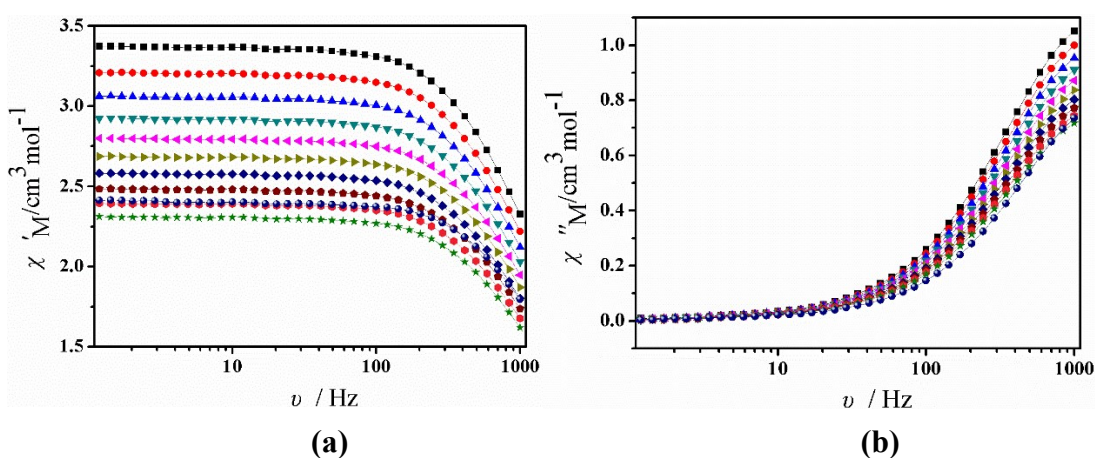


Fig. S18 Plots of the frequency-dependent in-phase (a) and out-of-phase (b) ac susceptibility at indicated temperatures for **3**.

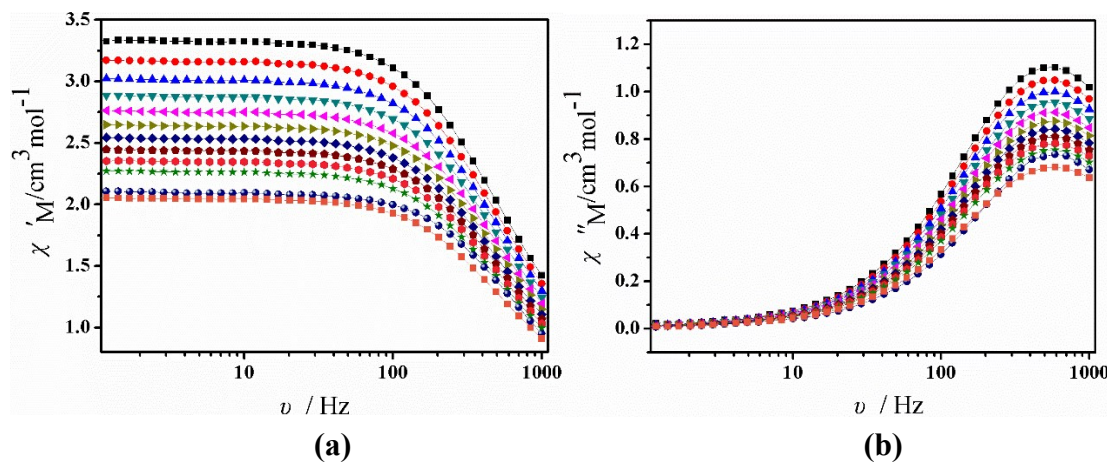


Fig. S19 Plots of the frequency-dependent in-phase (a) and out-of-phase (b) ac susceptibility at indicated temperatures for 4.

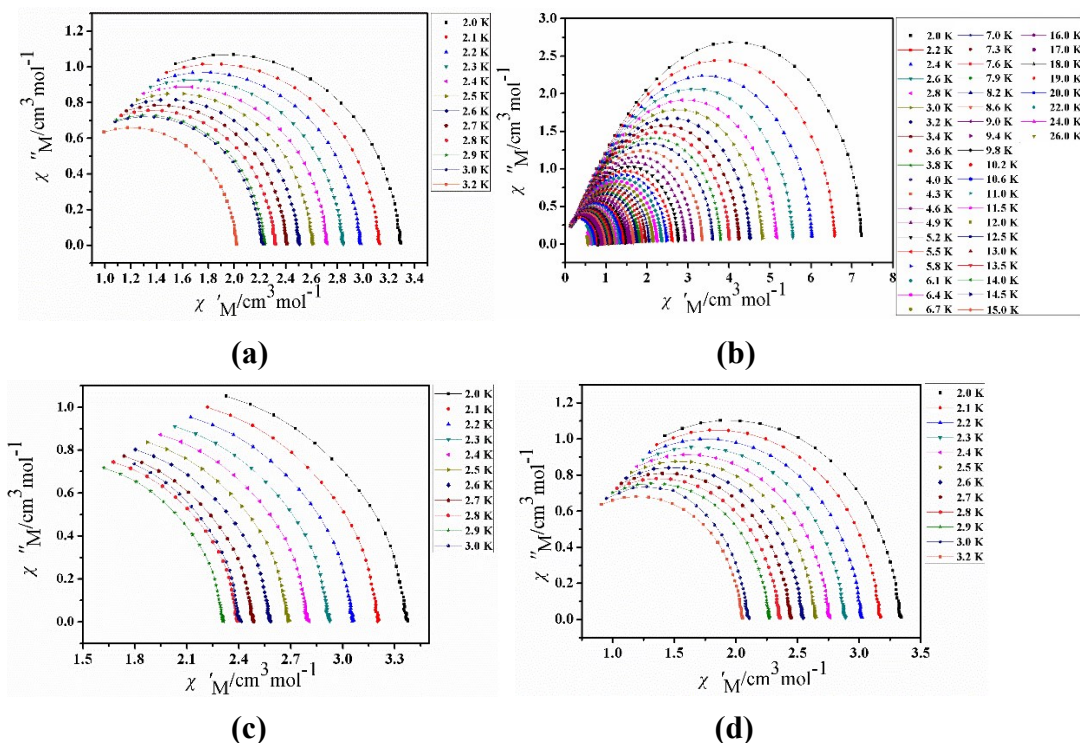


Fig. S20 Cole–Cole plots for **1–4** (a–d) using the ac susceptibility data under a zero applied dc field. The solid lines are guides for the eyes.

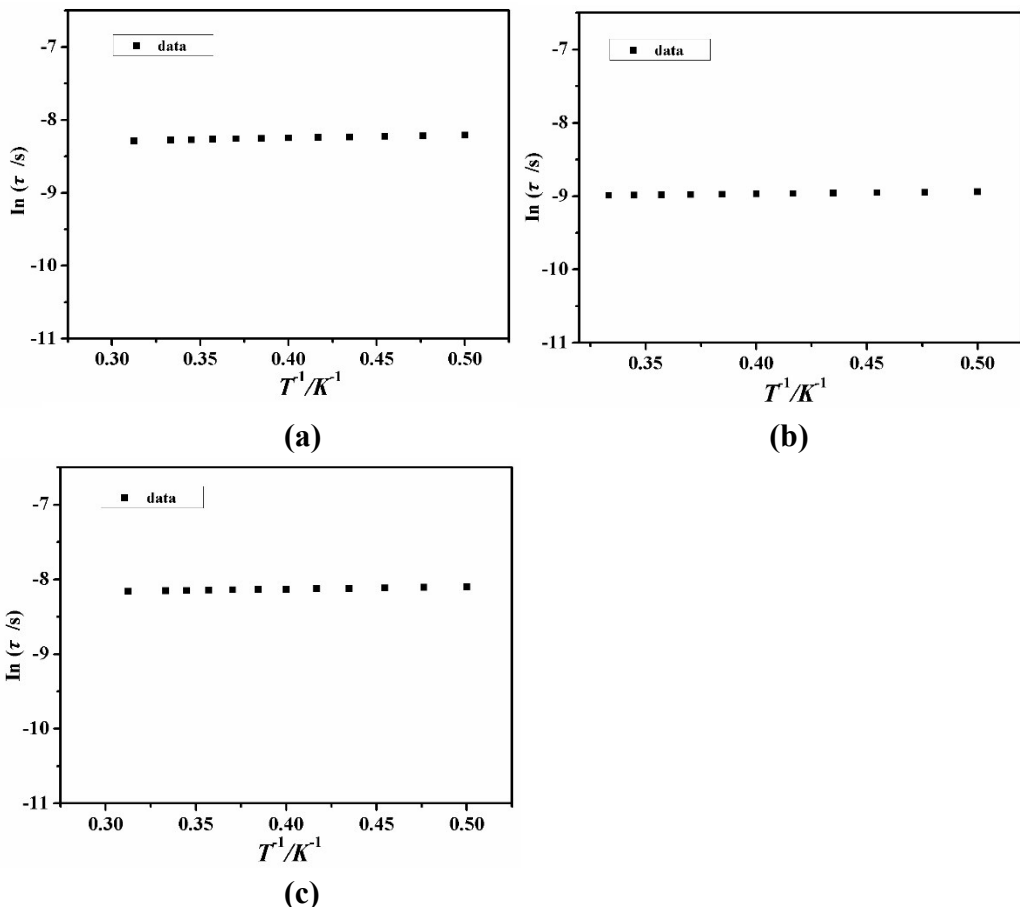


Fig. S21 Fitting of frequency dependence of relaxation time under 0 Oe dc field for **1**, **3** and **4**.

4. Relaxation fitting parameters of **1-4**

The magnetic susceptibility data of **1-4** under a zero dc field were described by the modified Debye functions:

$$\chi'(\omega) = \chi_s + (\chi_t - \chi_s) \frac{1 + (\omega\tau)^{1-\alpha} \sin(\frac{\pi}{2}\alpha)}{1 + 2(\omega\tau)^{1-\alpha} \sin(\frac{\pi}{2}\alpha) + (\omega\tau)^{(2-2\alpha)}}$$

$$\chi''(\omega) = (\chi_t - \chi_s) \frac{(\omega\tau)^{1-\alpha} \cos(\frac{\pi}{2}\alpha)}{1 + 2(\omega\tau)^{1-\alpha} \sin(\frac{\pi}{2}\alpha) + (\omega\tau)^{(2-2\alpha)}}$$

$$\chi''_{\omega=\tau^{-1}} = (\chi_t - \chi_s) \frac{\cos(\frac{\pi}{2}\alpha)}{2 + 2 \sin(\frac{\pi}{2}\alpha)} = \frac{1}{2} (\chi_t - \chi_s) \tan \frac{\pi}{4} (1 - \alpha)$$

Table S6 Relaxation fitting parameters from Least-Squares Fitting of $\chi(\omega)$ data for **1** under a zero applied dc field.

T	$\Delta\chi_1$ (cm ³ mol ⁻¹)	$\Delta\chi_2$ (cm ³ mol ⁻¹)	τ (s)	α
-----	---	---	------------	----------

2.0	0.689507E+00	0.330175E+01	0.272019E-03	0.121927E+00
2.1	0.654505E+00	0.313673E+01	0.269514E-03	0.121753E+00
2.2	0.622448E+00	0.298931E+01	0.267417E-03	0.121643E+00
2.3	0.592090E+00	0.285226E+01	0.265310E-03	0.120750E+00
2.4	0.565953E+00	0.272934E+01	0.263504E-03	0.120347E+00
2.5	0.545876E+00	0.261635E+01	0.262002E-03	0.120185E+00
2.6	0.524118E+00	0.251238E+01	0.260193E-03	0.120534E+00
2.7	0.506196E+00	0.241579E+01	0.258999E-03	0.119724E+00
2.8	0.486381E+00	0.232655E+01	0.257279E-03	0.120004E+00
2.9	0.469421E+00	0.224416E+01	0.255909E-03	0.120125E+00
3.0	0.463331E+00	0.222649E+01	0.256353E-03	0.123747E+00
3.2	0.425470E+00	0.202691E+01	0.252088E-03	0.119711E+00

Table S7 Relaxation fitting parameters from Least-Squares Fitting of $\chi(\omega)$ data for **2** under a zero applied dc field.

T	$\Delta\chi_1$ (cm ³ mol ⁻¹)	$\Delta\chi_2$ (cm ³ mol ⁻¹)	τ (s)	α
2	0.487257E+00	0.735784E+01	0.208471E-02	0.151705E+00
2.2	0.440066E+00	0.669337E+01	0.209213E-02	0.152937E+00
2.4	0.401882E+00	0.612943E+01	0.209446E-02	0.153523E+00
2.6	0.369632E+00	0.565707E+01	0.209694E-02	0.154151E+00
2.8	0.341931E+00	0.525148E+01	0.209997E-02	0.154876E+00
3	0.318101E+00	0.490092E+01	0.210146E-02	0.155440E+00
3.2	0.298343E+00	0.459249E+01	0.210082E-02	0.155537E+00
3.4	0.279624E+00	0.431970E+01	0.210131E-02	0.156265E+00
3.6	0.261977E+00	0.407928E+01	0.210172E-02	0.156895E+00
3.8	0.243227E+00	0.386213E+01	0.209794E-02	0.158117E+00
4	0.230564E+00	0.366825E+01	0.209686E-02	0.158139E+00
4.3	0.213398E+00	0.340864E+01	0.209319E-02	0.158686E+00
4.6	0.198145E+00	0.318466E+01	0.208735E-02	0.159188E+00
4.9	0.185115E+00	0.299028E+01	0.208514E-02	0.159973E+00
5.2	0.173465E+00	0.281515E+01	0.207706E-02	0.160248E+00
5.5	0.161730E+00	0.266260E+01	0.206837E-02	0.161158E+00
5.8	0.153274E+00	0.252350E+01	0.205841E-02	0.160860E+00
6.1	0.143769E+00	0.239805E+01	0.204477E-02	0.161354E+00
6.4	0.137590E+00	0.228530E+01	0.203123E-02	0.160399E+00
6.7	0.130304E+00	0.218429E+01	0.201194E-02	0.160687E+00
7	0.125371E+00	0.208876E+01	0.199124E-02	0.158726E+00
7.3	0.119306E+00	0.200377E+01	0.196948E-02	0.158262E+00
7.6	0.114118E+00	0.192365E+01	0.194000E-02	0.156620E+00
7.9	0.109318E+00	0.184996E+01	0.190796E-02	0.154824E+00
8.2	0.104367E+00	0.178343E+01	0.187154E-02	0.153233E+00
8.6	0.998976E-01	0.169725E+01	0.181358E-02	0.148098E+00
9	0.946468E-01	0.162214E+01	0.175181E-02	0.144359E+00

9.4	0.889242E-01	0.155238E+01	0.167984E-02	0.140552E+00
9.8	0.844830E-01	0.148779E+01	0.160357E-02	0.135471E+00
10.2	0.792711E-01	0.142929E+01	0.152352E-02	0.131205E+00
10.6	0.743353E-01	0.137250E+01	0.143256E-02	0.125345E+00
11	0.697022E-01	0.132312E+01	0.134722E-02	0.121015E+00
11.5	0.630159E-01	0.126413E+01	0.123706E-02	0.115771E+00
12	0.565298E-01	0.121025E+01	0.112727E-02	0.110440E+00
12.5	0.499300E-01	0.116173E+01	0.102007E-02	0.105819E+00
13	0.433379E-01	0.111643E+01	0.917631E-03	0.101812E+00
13.5	0.365184E-01	0.107380E+01	0.821622E-03	0.983315E-01
14	0.291307E-01	0.103385E+01	0.729979E-03	0.951945E-01
14.5	0.213466E-01	0.998656E+00	0.647059E-03	0.943072E-01
15	0.134180E-01	0.965166E+00	0.570363E-03	0.931482E-01
16	0.493932E-13	0.906072E+00	0.440738E-03	0.911922E-01
17	0.659887E-13	0.851564E+00	0.340675E-03	0.819669E-01
18	0.120494E-12	0.804728E+00	0.258896E-03	0.763472E-01
19	0.232322E-12	0.761652E+00	0.193433E-03	0.714606E-01
20	0.271291E-12	0.724095E+00	0.142986E-03	0.709857E-01
22	0.360185E-12	0.657850E+00	0.769629E-04	0.668911E-01
24	0.521998E-12	0.603270E+00	0.442440E-04	0.503988E-01
26	0.137017E-11	0.557161E+00	0.293909E-04	0.115979E-01

Table S8 Relaxation fitting parameters from Least-Squares Fitting of $\chi(\omega)$ data for **3** under a zero applied dc field.

T	$\Delta\chi_1$ (cm ³ mol ⁻¹)	$\Delta\chi_2$ (cm ³ mol ⁻¹)	τ (s)	α
2.0	0.834159E+00	0.337502E+01	0.131152E-03	0.111392E+00
2.1	0.791676E+00	0.320984E+01	0.130192E-03	0.110862E+00
2.2	0.757520E+00	0.306267E+01	0.129734E-03	0.110311E+00
2.3	0.719100E+00	0.292484E+01	0.128720E-03	0.110278E+00
2.4	0.688381E+00	0.280102E+01	0.128085E-03	0.109449E+00
2.5	0.658837E+00	0.268752E+01	0.127444E-03	0.109528E+00
2.6	0.632367E+00	0.258242E+01	0.126836E-03	0.109557E+00
2.7	0.607762E+00	0.248505E+01	0.126219E-03	0.109398E+00
2.8	0.585965E+00	0.239482E+01	0.125754E-03	0.108948E+00
2.9	0.564873E+00	0.231101E+01	0.125190E-03	0.108947E+00
3.0	0.590341E+00	0.240599E+01	0.106969E-03	0.916067E-01

Table S9 Relaxation fitting parameters from Least-Squares Fitting of $\chi(\omega)$ data for **4** under a zero applied dc field.

T	$\Delta\chi_1$ (cm ³ mol ⁻¹)	$\Delta\chi_2$ (cm ³ mol ⁻¹)	τ (s)	α
2	0.606521E+00	0.334572E+01	0.303655E-03	0.130584E+00
2.1	0.577853E+00	0.317966E+01	0.301756E-03	0.130156E+00

2.2	0.551388E+00	0.302868E+01	0.299631E-03	0.129566E+00
2.3	0.526246E+00	0.289145E+01	0.297687E-03	0.129580E+00
2.4	0.504961E+00	0.276676E+01	0.296305E-03	0.129424E+00
2.5	0.485592E+00	0.265247E+01	0.294747E-03	0.128587E+00
2.6	0.466579E+00	0.254819E+01	0.293166E-03	0.128560E+00
2.7	0.449172E+00	0.245100E+01	0.291822E-03	0.128374E+00
2.8	0.433951E+00	0.236096E+01	0.290716E-03	0.127888E+00
2.9	0.417505E+00	0.227728E+01	0.289111E-03	0.128103E+00
3	0.380786E+00	0.210350E+01	0.287470E-03	0.101634E+00
3.2	0.379904E+00	0.205760E+01	0.285969E-03	0.126676E+00

Table S10 The fitting parameters of different relaxation mechanisms for eqn (1).

The fitting parameters	Meanings	Values
τ	the inverse of the ac frequency	/
T	the temperature of the maximum in the ac signal	2.0–26.0 K
U_{eff}	the effective energy barrier	200.89 K
k	Boltzmann's constant	1.380649×10^{-23} J/K
τ_{QTM}	the fitting parameter of the QTM process	0.0021 s
n	the fitting parameter of the Raman process	4.86
C	the fitting parameter of the Raman process	$0.002 \text{ s}^{-1} \text{ K}^{-4.86}$
τ_0	the fitting parameter of the Orbach process	2.50×10^{-8} s

Theoretical methods and computational details

This section is supposed to be included in ESI.

Multiconfigurational *ab initio* calculations, including spin-orbit coupling (SOC), were performed on the experimental structures of the complexes here to explore their SMM properties. This type of calculation includes two steps:¹ 1) a set of spin eigenstates, are obtained by the state-averaged (SA) CASSCF method; ² 2) the low-lying SOC states, i.e., Kramers doublets (KD) herein, are obtained by state interaction which is the diagonalization of the SOC matrix in the space spanned by the spin eigenstates from the first step. In the CASSCF step, the active space consisted of 9 electrons in 7 orbitals and all the spin eigenstates of 21 sextets were included. Due to the hardware limitation, other highly excited quartets and doublets were not considered. The step of state

interaction were performed by the RASSI-SO module³ with the SOC integrals from the AMFI method.⁴ The ANO-RCC basis sets,^{5–7} including VTZP for Dy, VDZ for C and H as well as VDZP for other atoms, were used. All the calculations were carried out with the MOLCAS@UU, a version of MOLCAS 8.0^{8,9} which is freely distributed for academic users. The SINGLE ANISO module,^{10,11} developed by Chibotaru and et al, was used to obtain the g-tensors, transition magnetic moments and other parameters characterizing the magnetic anisotropy.

Table S11 Experimental and theoretically calculated τ_{QTM} (in s) of the compounds here.

	τ_{QTM}^{exp}	τ_{QTM}^{Zee}	Δlog_c
1	2.72×10^{-4} (-3.56) ^d	3.34×10^{-4} (-3.48)	0.08
2	2.10×10^{-3} (-2.86)	6.47×10^{-3} (-2.19)	0.49
3	1.31×10^{-4} (-3.88)	1.52×10^{-4} (-3.82)	0.06
4	3.04×10^{-4} (-3.52)	3.52×10^{-4} (-3.45)	0.07

^a τ_{QTM}^{exp} of **1**, **3** and **4** are taken as the relaxation time at 2 K. ^b B_{ave} is set to be 50 mT.

^c $\Delta log = log(\tau_{QTM}^{Zee}) - log(\tau_{QTM}^{exp})$. ^d logarithmic values are shown in parentheses.

REFERENCES

- [1] Javier Luzón and Roberta Sessoli. Lanthanides in molecular magnetism: so fascinating, so challenging. *Dalton Trans*, 41:13556–13567, 2012.
- [2] Björn O. Roos, Peter R. Taylor, and Per. E. M. Siegbahn. A COMPLETE ACTIVE SPACE SCF METHOD (CASSCF) USING A DENSITY MATRIX FORMULATED SUPER-CI APPROACH. *Chem Phys*, 48:157–173, 1980.
- [3] Per-åke Malmqvist, Björn O. Roos, and Bernd Schimmelpfennig. The restricted active space (RAS) state interaction approach with spin-orbit coupling. *Chem Phys Lett*, 357:230–240, 2002.
- [4] Bernd A Hess, Christel M Marian, Ulf Wahlgren, and Odd Gropen. A mean-field spin-orbit method applicable to correlated wavefunctions. *Chem Phys Lett*, 251:365–371, 1996.
- [5] Björn O. Roos, Roland Lindh, Per-åke Malmqvist, Valera Veryazov, and Per-Olof Widmark. Main Group Atoms and Dimers Studied with a New Relativistic ANO Basis Set. *J Phys Chem A*, 108(15):2851–2858, 2004.
- [6] Björn O. Roos, Roland Lindh, Per-åke Malmqvist, Valera Veryazov, and Per-Olof Widmark. New Relativistic ANO Basis Sets for Transition Metal Atoms. *J Phys Chem A*, 109(29):6575–6579, 2005.
- [7] Björn O. Roos, Roland Lindh, Per-åke Malmqvist, Valera Veryazov, Per-Olof Widmark, and Antonio Carlos Borin. New Relativistic Atomic Natural Orbital Basis Sets for Lanthanide Atoms with Applications to the Ce Diatom and LuF₃. *J Phys Chem*

- A*, 112(45):11431–11435, 2008.
- [8] HAMILTONIANS OF ANISOTROPIC MAGNETIC COMPLEXES. *Adv Chem Phys*, 153:397–519, 2013.
- [9] Francesco Aquilante, Luca De Vico, Nicolas Ferré, Giovanni Ghigo, Per-åke Malmqvist, Pavel Neogrády, Thomas Bondo Pedersen, Michal Pitoňák, Markus Reiher, Björn O. Roos, Luis Serrano-Andrés, Miroslav Urban, Valera Veryazov, and Roland Lindh. Molcas 7: The next generation. *J Comput Chem*, 31(1):224–247, 2010.
- [10] Francesco Aquilante, Jochen Autschbach, Rebecca K. Carlson, Liviu F. Chibotaru, Mickael G. Delcey, Luca De Vico, Ignacio Fdez. Galván, Nicolas Ferré, Luis Manuel Frutos, Laura Gagliardi, Marco Garavelli, Angelo Giussani, Chad E. Hoyer, Giovanni Li Manni, Hans Lischka, Dongxia Ma, Per-åke Malmqvist, Thomas Müller, Artur Nenov, Massimo Olivucci, Thomas Bondo Pedersen, Daoling Peng, Felix Plasser, Ben Pritchard, Markus Reiher, Ivan Rivalta, Igor Schapiro, Javier Segarra-Martí, Michael Stenrup, Donald G. Truhlar, Liviu Ungur, Alessio Valentini, Steven Vancoillie, Valera Veryazov, Victor P. Vysotskiy, Oliver Weingart, Felipe Zapata, and Roland Lindh. Molcas 8: New capabilities for multiconfigurational quantum chemical calculations across the periodic table. *J Comput Chem*, 37(5):506–541, 2016.
- [11] Liviu F Chibotaru and Liviu Ungur. Ab initio calculation of anisotropic magnetic properties of complexes. I. Unique definition of pseudospin Hamiltonians and their derivation. *J Chem Phys*, 137:064112, 2012.